Final call for paper

MWP/APMP 2014 SAPPORO

2014 International Topical Meeting on Microwave Photonics /
The 9th Asia-Pacific Microwave Photonics Conference (MWP / APMP 2014)

MWP/APMP 2014

20-23 October 2014 Sapporo Convention Center, Sapporo, Japan

Submission deadline (extended) : 26 May 2014

http://www.mwp2014.com

Conference scope:

- Optical technologies for high-frequency wireless systems
- Photonic techniques for microwave backhaul
- Photonic systems for antennas and beam forming
- Photonic systems based on non-binary signals
- MIMO technologies for microwave photonics
- Microwave photonic technologies for biomedical applications
- High-speed and/or broadband photonic devices
- Integration technologies for microwave photonic devices
- Optical analog-to-digital converters
- Optical probing and sensing of microwave fields or properties
- Optical generation of RF, microwave, millimeter-wave and THz waves
- Optical processing and control of analog and digital signals
- Novel device/technology for microwave photonics
- Innovative applications of microwave photonics

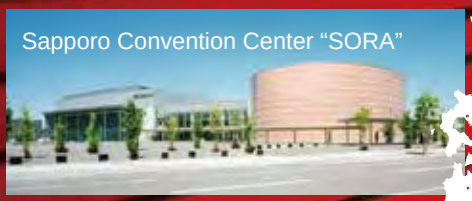

Sponsored by

IEICE Electronics Society

MTT-S® IEEE Microwave Theory and Techniques Society

IEEE photonics SOCIETY IEEE Photonics Society

The Telecommunications Advancement Foundation

NICT International Exchange Program

●Please click on the Sessions to jump to each pages.

MWP APMP 2014 Program at a Glance

Time	Oct. 20 (Mon)	Oct. 21 (Tue)	Oct. 22 (Wed)	Oct. 23 (Thu)
9:00		9:00 - 10:15		
		TuA Plenary & Invited Paper Session 1	**WA** Plenary & Invited Paper Session 2	**ThA** Plenary & Invited Paper Session 3
10:15		Coffee break		
10:45		10:45 - 12:15		
		TuB RoF for Mobile Communication Systems	**WB** MWP Sensing Technology	**ThB** High-Speed Photo-Detector & Optical Modulator
12:15	12:45 - 15:00	Lunch break @ Room 201 & 202		
13:45	**Workshop-1** "Advanced Photonics & MWP"	13:45 - 15:45		13:45 - 15:00
		TuC MWP integrated devices	**WC** THz Technology	**ThC** Novel RoF Technology
				15:00 - 15:30
	Coffee break			**ThD** Post Deadline
	15:30 - 18:00			Closing session
15:45		Coffee break		
16:15	**Workshop-2** "Asia-Pacific Microwave Photonics"	16:15 - 18:00		
		TuD Advanced Signal Processing Technology	**WD** Beam Forming & Related Technology	
18:00	18:00 - 20:00	18:00- 21:00		
	Get Together party @Restaurant SORA	**TuE Poster Session & Reception** @Room 206 & 207	19:30 - 21:30 **Banquet** @Sapporo Grand Hotel	

Oral Session (Plenary:45min, Invited:30min, Regular:15min) @Small Hall

TuEB-9 Crosstalk Reduction for Large Scale Photonic Integrated Circuits

Tuptim Angkeaw, Toshimasa Umezawa*, Tetsuya Kawanishi*, *Chulalongkorn University, Thailand*, **National Institute of Information and Communications Technology, Japan*

The fundamental crosstalk characteristics related to design of highly compact optical and RF signal lines has been studied in this work. The systematically investigation of the optical crosstalk of two parallel optical waveguides are carried out by modal analysis and the beam propagation analysis. The new idea of crosstalk mitigation in PIC by using uniform air gap along the longitudinal structure has been proposed. The crosstalk mitigation up to - 40dB by using air gap can successfully achieve, which results in reduction of spacing between signal lines.

TuEB-10 Development of Lumped Constant Type LN Optical Modulators Operating at 10GHz Band

Yoshikazu Toba, Kazuhisa Haeiwa*, Takeshi Kamio*, Hisato Fujisaka*, *SEIKOH GIKEN Co., Ltd., Japan*, **Hiroshima City University, Japan*

In order to create a lumped-constant LN (LiNbO3) optical modulator that operates with high sensitivity in the 7-10 GHz band, it is necessary to ascertain the impact of the electrode pad capacitance, lead inductance, and other factors. An electro-magnetic-field simulator has thus shown that the width of the LN crystal substrate is the main impediment to achieving high frequency and sensitivity; based on this result, we created four prototype 10-GHz band lumped-constant LN optical modulators, and evaluated their performance. As a result, we measured a resonant frequency of about 10.1GHz with an LN crystal substrate that was 1.4 mm wide and 0.3 mm thick, and achieved a 20dB CNR. This provided an optimistic outlook on the possibility of achieving a high-sensitivity LN optical modulator operating in the 10 GHz band, which is the highest allocated frequency range.

TuEB-11 An Equivalent Circuit Model for Germanium Waveguide Vertical Photodetectors on Si

Jeong-Min Lee, Woo-Young Choi, *Yonsei University, Korea*

We present an equivalent circuit model for 1.55-μm germanium waveguide vertical photodetector on a Si-on-Insulator (SOI) substrate. The model has two current sources for modeling photogenerated carriers so that those carriers experiencing drift and diffusion within the Ge intrinsic layer can be independently modeled. The model provides photodetection frequency response simulation results that match very well with the measurement results. It should be very useful for designing integrated Si optical receiver.

TuEB-12 Data Rate Penalty for High-Density Photonic Integrated Circuits in Advanced Modulation Formats

Toshimasa Umezawa, Tetsuya Kawanishi Tuptim Angkeaw*, *National Institute of Information and Communications Technology, Japan,*Chulalongkorn University, Thailand*

We report on a simulation investigation of the effects of signal lines and core pitch on RF and optical crosstalk in integrated photonic circuits, and we discuss the data rate with photonic circuit density in advanced modulation formats such as 64QAM.

TuEC: Optical generation of RF/MW/MMW/THz-waves

TuEC-1 Tunable Opto-Electronic Oscillator based on a Fiber-Ring Resonator and a Dual-Frequency Laser

Grégoire Pillet, Jérémy Maxin, Hadrien Lanctuit, Pascale Nouchi, Daniel Dolfi, Olivier Llopis*, Loïc Morvan, *Thales Research and Technology, France*, **LAAS-CNRS, France*

An Equivalent Circuit Model for Germanium Waveguide Vertical Photodetectors on Si

Jeong-Min Lee and Woo-Young Choi
Department of Electrical and Electronic Engineering, Yonsei University
50 Yonsei-ro, Seodaemun-gu, Seoul 120-749, Korea
minlj@yonsei.ac.kr

***Abstract*—We present an equivalent circuit model for 1.55-μm germanium waveguide vertical photodetector on a Si-on-Insulator (SOI) substrate. The model has two current sources for modeling photogenerated carriers so that those carriers experiencing drift and diffusion within the Ge intrinsic layer can be independently modeled. The model provides photodetection frequency response simulation results that match very well with the measurement results. It should be very useful for designing integrated Si optical receiver.**

Keywords*—Equivalent circuit model, germanium photodetector, optical interconnect, silicon photonics.

I. Introduction

There is a great amount of research interests for Si photonics as it promises solutions for the interconnect bottleneck problem that high-performance Si systems face [1]. In particular, high-performance monolithic optical receivers based on silicon photonics are actively investigated for 1.55-μm short-distance optical-communication and optical-interconnect applications [2]. Germanium photodetectors having high responsivity and large bandwidth have been reported that can be integrated with silicon waveguides using vertical [3], [4], lateral [5] p-i-n, and MSM [6] structures. In order to realize integrated optical receivers based on these PDs, accurate equivalent circuit models are necessary so that the entire optical receiver can be designed in a unified manner based on the conventional electronic circuit design environment.

In this paper, we introduce a new equivalent circuit model for Ge waveguide vertical PDs (Ge-VPDs) realized on a Si-on-Insulator (SOI) wafer. This model has two separate current sources so that photogenerated carrier dynamics due to drift and diffusion can be independently modeled. The electric-field profiles at different bias voltages for our target Ge-VPDs are simulated and, from this, key model parameter values are determined. Our model shows well-matched photodetection frequency responses to the measurement results at different reverse bias voltages.

II. Structure and Equivalent Circuit Model

The Ge-VPD under investigation is fabricated on 220-nm thick SOI layer having 2-μm thick buried-oxide layer (BOX) on Si substrate. The device fabrication is done through the OpSIS-IME Si photonics multi-project wafer service [7]. Fig. 1

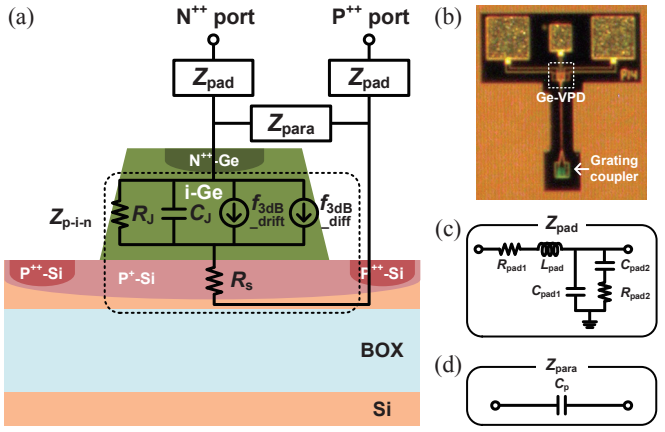

Fig. 1. (a) Cross-section and equivalent circuit model for Ge-VPD. (b) Top view of the fabricated Ge-VPD. (c) Equivalent circuit model for pads and interconnection lines. (d) Equivalent circuit model for the parasitic elements.

shows the device structure as well as the equivalent circuit model used for our investigation. The thickness, width, and length of the Ge layer on SOI are 0.5, 8, and 11 μm, respectively. The vertical p-i-n junction is formed by p-type silicon (P^+-Si), intrinsic Ge (i-Ge) and highly doped n-type germanium (N^{++}-Ge) layers. As shown in Fig. 1(b), light is coupled into the Si waveguide through a grating coupler and then introduced into the Ge-VPD.

The equivalent circuit model includes $Z_{p\text{-}i\text{-}n}$, Z_{pad}, and Z_{para} as shown in Fig. 1(a). $Z_{p\text{-}i\text{-}n}$ represents P^+-Si/i-Ge/N^{++}-Ge junction. In $Z_{p\text{-}i\text{-}n}$, C_J and R_J are the depletion capacitance and drift region resistance, respectively. R_s is the series resistance of the inactive region. In addition, two current sources having single-pole frequency responses with f_{3dB_drift} and f_{3dB_diff} represent photogenerated carriers that experience drift in the depletion region and diffusion in the undepleted region, respectively. When a p-i-n diode is fully depleted, photogenerated carriers experience drift. However, in our Ge-VPD, there exists a region which is not completely depleted due to the device structure. The existence of the undepleted region can be observed from Fig. 2, which shows the simulated electric-field profiles for Ge-VPD at two different bias voltages of -1 V and - 4 V. The simulation is done with Synopsis TCAD Sentaurus Device using doping profiles provided by the foundry service. As can be seen in Fig. 2, there is a region near the Ge waveguide edges where the electric-field is not strong

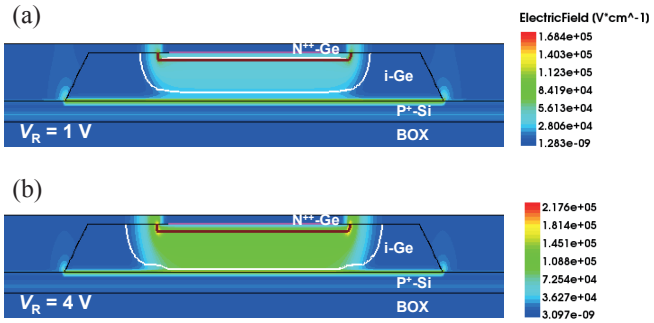

Fig. 2. Simulated electric-field profiles for Ge-VPD (a) at 1-V and (b) at 4-V reverse bias voltage.

enough for depletion. Consequently, photogenerated carriers experience both fast drift and slow diffusion, influencing the overall photodetection frequency response.

II. Measurement and Parameter Extraction

For measurement, light from a 1.55-μm CW laser is injected into the grating couplers through single-mode lensed fiber and output electrical signals are measured through high-speed RF probes. Illumination optical power is about -2 dBm and bias voltages are applied to Ge-VPD through a bias-tee. The lightwave component analyzer is used for measuring electrical *S*-parameters as well as photodetection frequency responses. Open and short test patterns are fabricated on the same wafer to extract Z_{pad} parameter values.

For $Z_{p\text{-}i\text{-}n}$, C_J can be determined from the known equation, $C_J=\varepsilon_{Ge}A/W_D$. C_J, R_J and R_s are determined by fitting the simulated reflection coefficients to the measured results using Agilent Advanced Design System. Fig. 3 shows the measured and fitted simulated results.

f_{3dB_drift} is determined to be $0.45\times v_{sat}/W_D$, using depletion width, W_D, and saturation velocity, v_{sat} of Ge [8]. To calculate f_{3dB_diff}, the doping levels of 5×10^{15} cm^{-3} is assumed for i-Ge and hole diffusion coefficient (D_p) is about 40 cm^2/s. The hole diffusion time constant is calculated to be about 25.3 ps. From these, f_{3dB_drift} and f_{3dB_diff} are determined 54 GHz and 6.28 GHz, respectively. Values for the extracted parameters are listed in Table I.

Fig. 4 shows the measured and simulated photodetection frequency responses at two different reverse bias voltages. For the simulation, our equivalent circuit model with extracted circuit parameter values is used. As can be seen, the matching is good, confirming the accuracy of our model. At the reverse bias voltage of 1 V, more photogenerated carriers experience diffusion and the RC time constant is larger, resulting in smaller photodetection bandwidth than that of 4 V.

III. Conclusion

We present an equivalent circuit model for Ge-VPD fabricated on SOI. Our model includes two separate current sources for photogenerated carriers experience drift and diffusion. Two current sources are used because we identify

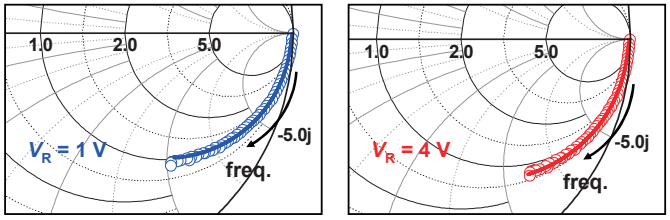

Fig. 3. Measured and fitted reflection coefficients for Ge-VPD from 50 MHz to 40 GHz at 1 and 4-V reverse bias voltages. Hollow circles represent the measurement results and solid lines as the simulation results.

TABLE I. Extracted Parameters for Z_{PAD}, Z_{PARA}, and $Z_{P\text{-}I\text{-}N}$

	Z_{pad}, Z_{para}		$Z_{p\text{-}i\text{-}n}$ at -1V	$Z_{p\text{-}i\text{-}n}$ at -4V
L_{pad} [pH]	65	R_s [Ω]	130	120
R_{pad1} [Ω]	1.1	C_J [fF]	18	15
R_{pad2} [kΩ]	20	R_J [kΩ]	17	
C_{pad1} [fF]	4.35	f_{3dB_drift} [GHz]	54	
C_{pad2} [fF]	6.1	f_{3dB_diff} [GHz]	6.28	
C_p [fF]	6			

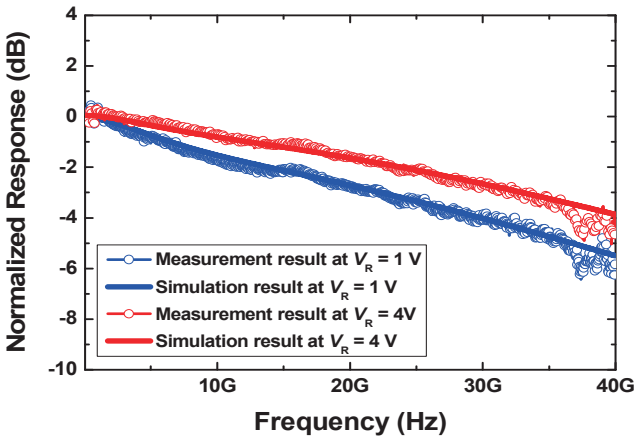

Fig. 4. Measured and simulated photodetection frequency responses for Ge-VPD from 50 MHz to 40 GHz at 1 and 4-V reverse bias voltages. Hollow circles represent the measurement results and solid lines as the simulation results.

from TCAD simulation that there are undepleted regions in our Ge-VPD. We confirm the accuracy of our model by comparing the model simulation results with the measurement results. We believe our equivalent circuit model is very useful for designing high-performance monolithic optical receivers.

Acknowledgment

This work was supported by the National Research Foundation of Korea (NRF) grant funded by the Korea government (MEST) (2012R1A2A1A01009233).

References

[1] L. C. Kimerling *et al.*, "Electronic-photonic integrated circuits on the CMOS platform," *Proceedings of SPIE*, vol. 6125, pp. 612502-612511, Mar. 2006.

[2] J. F. Buckwalter *et al.*, "A Monolithic 25-Gb/s Transceiver With Photonic Ring Modulators and Ge Detectors in a 130-nm CMOS SOI Process," *IEEE Journal of Solid-State Circuits*, vol. 47, no. 6, pp. 1309-1322, June 2012.

[3] A. Novack *et al*., "Germanium photodetector with 60 GHz bandwidth using inductive gain peaking," *Optics Express*, vol. 21, no. 23, pp. 28387-28393, Nov. 2013.

[4] L. Vivien *et al*., "42 GHz p.i.n Germanium photodetector integrated in a silicon-on-insulator waveguide," *Optics Express*, vol. 16, no. 8, pp. 6252-6257, Apr. 2009.

[5] G. Dehlinger *et al*., "High-Speed Germanium-on-SOI Lateral PIN Photodiodes," *IEEE Photonics Technology Letters*, vol. 16, no. 11, pp. 2547-2549, Nov. 2004.

[6] L. Vivien *et al*., "Metal-semiconductor-metal Ge photodetectors integrated in silicon waveguides," *Applied Physics Letters*, vol. 92. no. 15, p. 151114, 2008.

[7] Y. Zhang *et al*., "Silicon Multi-Project Wafer Platforms for Optoelectronic System Integration," *2012 IEEE 9th International Conference on Group IV Photonics*, pp. 63-65, Aug. 2012.

[8] S. M. Sze, Physics of Semiconductor Devices, 3rd ed. New York: Wiley, ch. 13, 2007.